

Progress in fast and red plastic scintillators

Matthieu Hamel

▶ **To cite this version:**

Matthieu Hamel. Progress in fast and red plastic scintillators. Chemosensors, 2022, 10 (2), pp.86. 10.3390/chemosensors10020086 . cea-03582648

HAL Id: cea-03582648
https://cea.hal.science/cea-03582648

Submitted on 21 Feb 2022

HAL is a multi-disciplinary open access archive for the deposit and dissemination of scientific research documents, whether they are published or not. The documents may come from teaching and research institutions in France or abroad, or from public or private research centers.

L'archive ouverte pluridisciplinaire **HAL**, est destinée au dépôt et à la diffusion de documents scientifiques de niveau recherche, publiés ou non, émanant des établissements d'enseignement et de recherche français ou étrangers, des laboratoires publics ou privés.



Distributed under a Creative Commons Attribution 4.0 International License

Progress in fast and red plastic scintillators

Matthieu Hamel

Université Paris-Saclay, CEA, List, F-91120 Palaiseau, France

matthieu.hamel@cea.fr; Orcid number 0000-0002-3499-3966

Abstract

Radiological detection where Cherenkov residual background can be prominent requires scintillators with increased emission wavelength. Cherenkov residual background precludes the use of UV-emitting sensors such as plastic scintillators. However, the literature is scarce in red-emitting plastic scintillators and only one commercial scintillator is currently available (BC-430, from Saint-Gobain Crystals and Detectors). In addition, X-ray imaging or Time-of-Flight Positron Emission Tomography (ToF-PET) applications are also demanding on this type (color) of scintillators, but only their scintillation decay time is fast, which is not particularly the case for BC-430. We present herein our latest developments in the preparation and the characterization of fast and red plastic scintillators for this application. Here "fast" means nanosecond range decay time and "red" is an emission wavelength shifted towards more than 550 nm. At first, the strategy to the preparation of such material is explained by decomposing the scintillator to fundamental elements. Each stage is then optimized in terms of decay time response, then the elemental bricks are arranged to give plastic scintillator formulations that are compatible with the abovementioned characteristics. The results are compared with the red-emissive BC-430 commercial plastic, and the ultra-fast, violet-emitting BC-422Q 1% plastic.

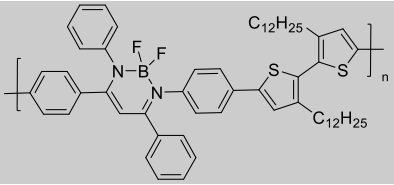
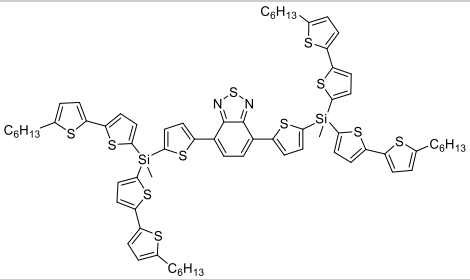
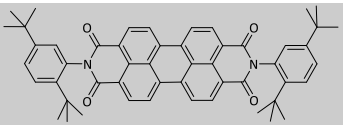
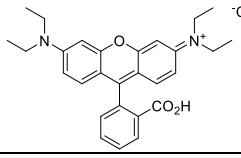
1. Introduction

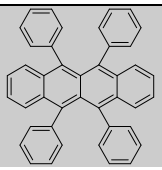
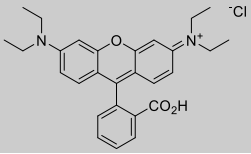
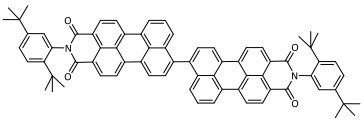
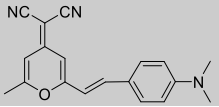
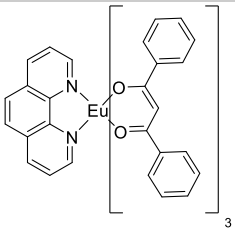
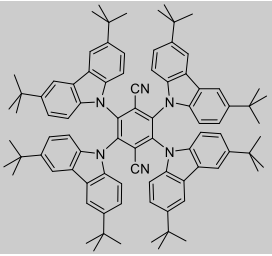
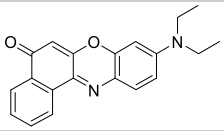
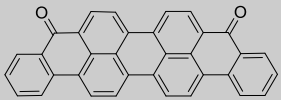
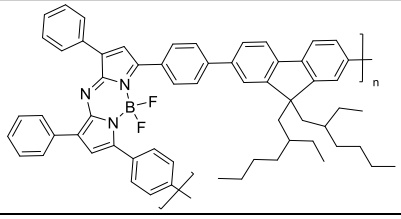
Various nuclear experiments are seeking to new detectors. The quest for new particles or improved detection efficiency is a trade-off with more constraints, thus pushing to garbage standard, yet efficient detectors, to be replaced by new, application-driven detectors. This is the place where material chemists step in, at least in the world of nuclear instrumentation. Among the possible emission-wavelength variations of scintillators, red emitters are probably the ones with the less demand.[1] Everybody knows and uses scintillators with standard emission wavelength, that is to say emitting close to 425 nm. Green-emitting plastic scintillators are useful when coupling to silicon photodiodes has to be achieved or when radiation-hard materials are necessary.[2] This being said, red-emitting scintillators are not commonly studied in this field, despite the fact they find relevant applications in physics domains, such as in the study of transient nuclear phenomena.[3] Other examples are noteworthy where Cherenkov residual may become an issue: plastic scintillator dosimetry (PSD),[4] ToF-PET, real time X-ray imaging and high-energy physics such as the Laser Mégajoule.[5]

The Cherenkov radiation spectrum is continuous and its intensity is inversely related to the square of the wavelength. So as to reduce or even avoid it in the counting of the incident dose rate, it is thus necessary to work with wavelengths usually more than 550 nm. Table 1 summarizes some scintillators of interest and their main properties.[6] YAG:Ce is the only inorganic scintillator given for comparison. Its main drawback is the long decay time that precludes its use when fast counting or timing resolution

is needed. BC-430 plastic scintillator is red-emitting and has a good light yield but still its decay time might be too long for the given applications. To the best of our knowledge, the first red-emitting scintillator reported in the literature has been prepared by Berlman and Ogdan.[7] This material was composed of a photonic cascade starting with 2-([1-biphenyl]-4-yl)-5-(*p*-*tert*-butylphenyl)-1,3,4-oxadiazole (butyl-PBD), 1,4-bis(5-(*o*-tolyl)oxazol-2-yl)benzene (dimethylPOPOP), perylene and rubrene, all these fluorophores being hosted in polystyrene. Their trick was to irradiate the scintillator with electrons created from a LINAC, thereby reducing the 35 ns preliminary decay time down to 5 ns only by molecular degradation. However, the scintillator revealed to recover from irradiation (as they use to be[8]) and the decay time increased accordingly. Since this seminal paper, several strategies have been tested towards the preparation of new red-emitting plastics (Table 1), with the use of organic fluorophores showing high-range aromaticity or internal Förster energy transfer, organometallics, BODIPY or xanthene derivatives, or more recently with organic molecules showing Thermally Activated Delayed Fluorescence (TADF). Noteworthy, our laboratory published some years ago their preliminary results on such chemical modifications for new red and fast plastics.[9] Thus, a polystyrene-based scintillator including 2,5-diphenyloxazole, Nile red and piperidine as the quencher displayed low scintillation yield and moderate decay time but at high wavelength (more than 600 nm). This publication presents our latest results on this field. It is decomposed as follows. The choice of the primary and the secondary fluorophores was performed independently, then ternary mixtures (matrix + primary fluorophore + secondary fluorophore) were studied, eventually with the addition of a photoluminescent quencher.

Table 1. Main plastic and liquid scintillators. Only scintillators operating at $\lambda_{em}^{max} > 550\ nm$ are cited. The list is sorted in ascending emission wavelength.

State	Last fluorophore	λ_{em}^{max} (nm)	Light output (ph/MeV)	Decay time (ns)[c]	Ref.
YAG:Ce	$Y_3Al_5O_{12}(Ce)$	550	8000	70	-
PVT scintillator	BC-430	580	6900	16.8	-
Polymer thin film		584	n.d.	0.46 (60) + 1.0 (40)	10
Polystyrene scintillator		588	9780	n.d.	11
Polystyrene scintillator		591	80	9.22-13.26	5
Polystyrene scintillator		595	n.d.	5.94	12

Polystyrene scintillator		> 600	n.d.	5	7
Polysiloxane scintillator	Lumogen Red	≈ 600	8300	n.d.	13
Polystyrene scintillator		600	≈ 16000	≈ 6	3
PMMA scintillator	$CsPbBr_3$ Perovskite + 	≈ 600	≈ 9000	3.4 (87) + 14.1 (13)	14
Poly(styrene-co-acrylonitrile) scintillator		≈ 610	n.d.	n.d.	15
Polystyrene scintillator		614	5650[b]	469000	16
Sucrose octaacetate		618	37500	10.9 + 1960	17
Polystyrene scintillator		610-620	70-300	8.7	9
PMMA scintillator		≈ 620	n.d.	3.94	18
Polymer in liquid		750	n.d.	1.92	19

[a] *n.d. not determined*

[b] *value obtained from ^{239}Pu alpha excitation*

[c] *usually monoexponential. When it is biexponential, it is expressed at the percentage of the first and the second exponential in the global fit.*

2. Experimental

Materials

All chemicals were purchased from Sigma-Aldrich, except for PMP and *p*-sexiphenyl that were obtained from TCI Europe Research Chemicals. Styrene and vinyltoluene were distilled prior to use. 4-Bromo-*p*-terphenyl was prepared according to a published procedure;[20] a white powder was obtained with an 80% yield after purification. *N*-(2-ethylhexyl carbazole) was prepared according to our previous work.[21] Spectroscopic toluene was obtained from Carlo Erba. BC-430 and BC-422Q 1 and 2% plastic scintillators were obtained from Saint-Gobain Crystals and Detectors; unfortunately, their purchase date is not known and one has to keep in mind that BC-422Q may suffer from aging with time.[22] All the monomers and amines were vacuum-distilled prior to the experiment. Liquid scintillators were prepared by dissolving the dyes into spectroscopic toluene. No other scintillation solvent was studied. Once prepared, the solutions were neither degassed nor saturated with neutral gas. The reason is twofold: the presence of oxygen decreases the decay time, and the saturation with neutral gas is modified by oxygen diffusion within the liquid. Plastic scintillators were prepared according to our internal procedure, except the fact that the monomers were not degassed prior to polymerization. After heating the monomer with the suitable molecules until complete polymerization, the raw material was cut and polished until obtaining a plastic scintillator with dimensions 49 mm diameter and 30 mm thickness (unless otherwise stated), which are in the same size range of BC-422Q 1% (Φ 50 mm, h 10 mm) or BC-430 (Φ 50 mm, h 50 mm) used as reference materials.

Methods

Fluorescence spectra were recorded with a Horiba Jobin Yvon Fluoromax 4P spectrofluorometer (Horiba Jobin Yvon) monitored with FluorEssence software. The fluorescence spectra were recorded orthogonally to the excitation light. The photoluminescence decay characteristics of the liquid and plastic scintillators were investigated with the Time-Correlated Single Photon Counting (TCSPC) module available as an option on this device. Two different excitation wavelengths were used, 274 nm and 368 nm, with pulse widths < 1.2 ns. In liquid state, TCSPC analyses were performed in standard 1 x 1 x 3 cm^3 quartz cuvettes with the emission recorded at 90° from the excitation diode. Plastic scintillators were excited on their cylindrical edge, the flat face being directed toward the photodetector of the spectrofluorometer. Decay spectra were fitted using the DAS6 software (Horiba Jobin Yvon). In each case, a biexponential fit was adjusted so that the χ^2 was in the range 1.00 – 1.20. The instrument response function was recorded by replacing the sample with a 3 cm^3 quartz cuvette filled with Ludox®. The mean decay times are given with two decimals, for a better comparison between the materials. Radioluminescence spectra were acquired according to our latest published experimental procedure[2] with a beta-emitting $^{90}Sr/^{90}Y$ source (31.9 MBq as of Nov. 2020).

The absorption characteristics of molecules were recorded with an Agilent Cary 60 UV-Vis spectrophotometer, with an optical path of 1 cm.

Pulse-height spectra were obtained as follows. In a black bow, the scintillator was coupled with optical grease to a blue-sensitive R6231 photomultiplier tube (Hamamatsu) or a red-sensitive 9202SB photomultiplier tube (ET Enterprises), depending on the scintillator to be tested, operating at -1100 V or -1700 V, respectively. The anode fed a DT5730SB digitizer from CAEN. A ^{137}Cs (gamma ray, 500 kBq as of Nov. 2020) located ca. 10 cm away from the scintillator or a ^{36}Cl source (6 kBq as of Nov. 2020) placed on the top of the scintillator were used, and the obtained pulse height spectrum was recorded during 500 seconds.

3. Results and discussion

Fast and red plastic scintillators can be decomposed into the following components: polymer, fluorophores and if necessary photoluminescence quencher. Each elemental brick was individually examined to allow a better understanding on possible limitations or improvements. Polystyrene or poly(vinyltoluene) were considered as the polymer building block since they are very well-known polymers and are the ones used in the composition of almost all commercial plastic scintillators.[1] No other polymers were considered in this study. In addition, thermally-assisted radical polymerization was used to polymerize the suitable, highly purified monomers.

To get more rationalization on the results and insight into each chemical's role, binary mixtures, that is to say matrix + primary fluorophore or matrix + secondary fluorophore were studied first. Each fluorophore has indeed its solvent-dependent photophysical properties (emission wavelength and more particularly herein decay time) and has to be experimentally assessed. The Holy Grail would be to have a fluorophore combination presenting the desired time characteristics, in other words without necessity to quench the photoluminescence with extra molecules. This would afford a highly scintillating, time-stable yet fast plastic scintillator.

It is noteworthy that the shape, the thickness and the coating of a scintillator have a large influence on its resulting decay time.[23] A 50% increase of the decay time constant can be observed when increasing the material's thickness from 0.2 to 5 cm.[24] The scintillator needs to be wrapped with black material to mitigate internal reflections. Intuitively thinner scintillators afford the best timing properties. The purpose of our work was to find out the best chemical composition; no morphology improvement was therefore performed. This is why each Table referencing timing properties of plastics mentions the diameter and the thickness of each material.

Intrinsic limitations of the spectrofluorometer setup

Our equipment uses two different Horiba Jobin Yvon NanoLED excitation sources that operates at either 274 nm or 368 nm (N-270 and N-370 LED heads, respectively) for Time-Correlated Single Photon Counting experiments. This constitutes the main limitation of this study since these two diodes display typical pulse widths less than 1.2 ns, so close to the best decay times we are currently measuring and expecting (and even higher than commercial references BC-422Q 1 and 2%).[25] One can see that the excitation profile is not purely monoexponential, with a bump appearing a few nanoseconds after the pulse. Their Full-Width at Half Maximum (FWHM) values are 1.48 ns ± 0.11 ns and 1.68 ns ± 0.11 ns. Without any access to better-resolved pulse diodes, the results are presented as such.

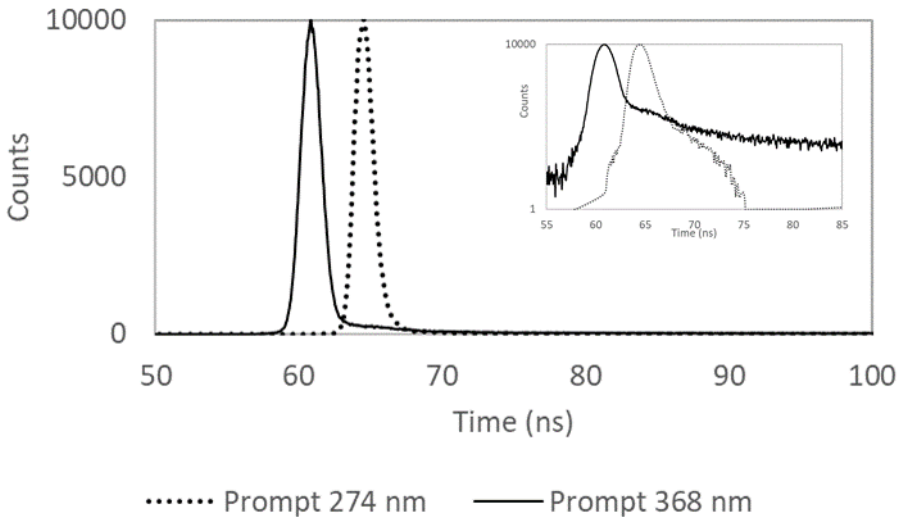
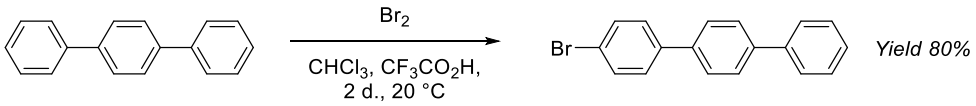


Figure 1 Excitation profiles of the two NanoLEDs used in this experiment, dashed line: 274 nm, solid line: 368 nm. Inset: focus on the afterpulses.

Matrix + primary fluorophore mixtures

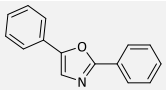
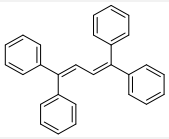
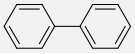
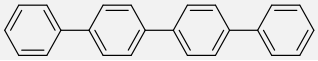
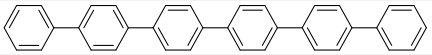
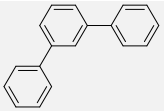
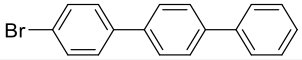
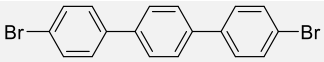
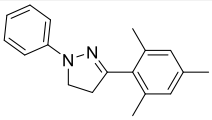
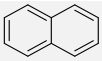
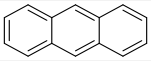
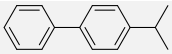
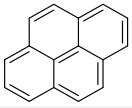
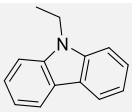
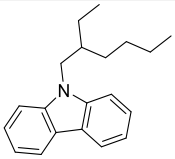
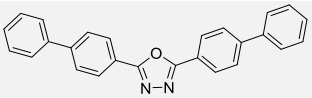
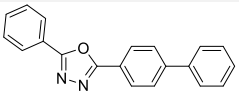
Such combinations have been widely documented and reviewed[24] by many pioneering works on plastic scintillator formulations. These so-called binary mixtures have proven to be the fastest decaying scintillators: adding a wavelength-shifter to the solution implies other energy transfers that can occur both radiatively and non-radiatively. So as to perform a fast screening, various molecules suitable for scintillation purpose were solubilized in toluene at 1 wt%, and their photoluminescence decay time was recorded by Time-Correlated Single Photon Counting (TCSPC) measurements.

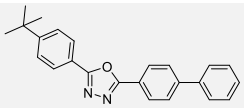
Among other strategies,[26] the intramolecular heavy atom quenching was assessed by adding one or two bromine atoms on the *para* positions of *p*-terphenyl. It seems that the fastest UV-emitting plastic scintillator ever described was prepared according to this approach.[27] Thus, 4-bromo-*p*-terphenyl was synthesized according to a published procedure.[20] Bromine reacted on *p*-terphenyl in a mixture of dichloromethane and trifluoroacetic acid and readily afforded 4-bromo-*p*-terphenyl with an 80% yield. The other tested molecules were used with commercial grade and no further purification. For all scintillators described thereafter, it is noteworthy that the solutions were not degassed so as to allow dissolved oxygen to act as a potential quencher of long-lived stated. The results of 19 different benchmarked molecules are given in Table 2. A non-linear fitting was chosen between single or biexponential decay so that the χ^2 fitting value was restricted to the range 1.00 – 1.20. Some of these molecules are known to display either a concentration-dependent (2,5-diphenyloxazole, *N*-(2-ethylhexyl)carbazole, pyrene) or an oxygen-sensitive (naphthalene, pyrene) decay time. Therefore, these results have to be considered as a fast qualitative survey of family of molecules that could be suitable to the foreseen application. The results show that phenylene- and PBD-derivatives are of particular interest in this context. In the oligophenylene series, the photoluminescence decay time shortens when increasing the number of phenyl groups, however at the expense of the solubility of the molecule.



Scheme 1 Preparation of 4-bromo-p-terphenyl

Table 2 Mono or biexponential fitting of the photoluminescence decay of molecules dissolved at 1 wt% in toluene (λ_{ex} = 274 nm; $\lambda_{obs} = \lambda_{em}^{max}$)

Molecule	Structure	Mono- or biexponential τ (ns)[a]	<τ> (ns)[b]
PPO		2.27	2.27
1,1,4,4-tetraphenylbutadiene		1.45 (99) + 34.7 (1)	1.78
Biphenyl		4.81	4.81
***p*-terphenyl**		1.45	1.45
***p*-quaterphenyl**		0.85 (73) + 1.82 (27)	1.11
***p*-sexiphenyl**		1.67 (66) + 2.83 (34)	2.06
***m*-terphenyl**		1.15 (59) + 8.96 (41)	4.35
4-bromo-*p*-terphenyl		0.72 (58) + 3.81 (42)	2.01
4,4′-dibromo-*p*-terphenyl		1.90 (64) + 12.54 (36)	5.73
***PMP* 1-phenyl-3-(mesityl)-2-pyrazoline**		4.11	4.11
Naphthalene		8.67	8.67
Anthracene		2.42 (90) + 8.51 (10)	3.03
4-isopropylbiphenyl		0.80 (5) + 4.94 (95)	4.73
Pyrene		23.0	23.0
***N*-ethylcarbazole**		7.91	7.91
***N*-(2-ethylhexyl)carbazole**		12.30	12.30
***BBD* 2,5-di(4′-biphenylyl)-1,3,4-oxadiazole**		1.35	1.35
***PBD* 2-phenyl-5-(4′-biphenylyl)-1,3,4-oxadiazole**		1.51	1.51

Butyl-PBD **2-(*p-tert*-butylphenyl-5-(4′-biphenylyl)-1,3,4-oxadiazole**		0.92 (54) + 1.64 (46)	1.25

[a] When the fitting of the decay curve proved to be better expressed as a biexponential, the results are given according to the following: τ_{fast} (%$_{fast}$) + τ_{slow} (%$_{slow}$).

[b] $\langle\tau\rangle = \tau_{fast} \times \%_{fast} + \tau_{slow} \times \%_{slow}$

A possible photoluminescence quenching of *p*-terphenyl and *p*-quaterphenyl with benzophenone or ternary, hindered amines was also tested with piperidine or *N,N*-diisopropylethylamine (also known as Hünig's base). At least in the toluene medium (Table 3), all three quenchers proved their efficiency with the best results observed for *p*-terphenyl quenched with piperidine. Thus, starting with already fast materials (τ = 1.76 and 1.73 ns for *p*-terphenyl and *p*-quaterphenyl, respectively), quenching leads to decay values close to 1 ns, so in the range of the instrument response function provided by the NanoLED characteristics (Figure 1). At this stage, no care was taken on the photoluminescence or even scintillation efficiency.

Table 3 Photoluminescence quenching of p-*terphenyl or* p-*quaterphenyl with piperidine or benzophenone in toluene. λ_{ex} = 274 nm; λ_{obs} = 342 nm (*p-*T) or 386 nm (*p-*Q)*

Molecule	Quencher (wt%)	τ (ns)	<τ> (ns)
***p*-terphenyl**	-	1.76	1.76
***p*-terphenyl**	Benzophenone (0.4)	0.59 (63.5) + 1.85 (36.5)	1.05
***p*-terphenyl**	Piperidine (1.6)	0.60 (71) + 1.92 (29)	0.98
***p*-terphenyl**	Hünig's base (1.6)	0.66 (78.6) + 2.11 (21.4)	0.97
***p*-quaterphenyl**	-	0.85 (73) + 1.82 (27)	1.11
***p*-quaterphenyl**	Benzophenone (0.4)	0.77 (42.5) + 2.08 (57.5)	1.52
***p*-quaterphenyl**	Piperidine (1.6)	1.73	1.73
***p*-quaterphenyl**	Hünig's base (1.6)	0.71 (48.5) + 4.44 (51.5)	2.6

We then turned our attention on binary plastic compositions of *p*-terphenyl, *p*-quaterphenyl and 4-bromo-*p*-terphenyl, these fluorophores being eventually quenched with benzophenone. Table 4 resumes the photoluminescence properties of various plastic scintillators compared with BC-422Q 1% and 2% commercial plastic scintillators. According to the literature, these scintillators are assumed to be quenched with benzophenone. All scintillators are still UV-emitters, with BC-422Q 2% and PS *p*-T 2 B 2 (see Table 4 for the interpretation of this abbreviation) which are the two scintillators emitting at wavelengths more than 400 nm. This effect might be related to the use of 2% of benzophenone that absorbs part of the emitted light below 400 nm.

Table 4 Photoluminescence properties of several plastic-state binary mixtures, eventually quenched with benzophenone. λ_{ex} = 274 nm; $\lambda_{obs} = \lambda_{em}^{max}$. All scintillators are with dimension Φ 49 mm h 10 mm

Composition*	Mono- or biexponential τ (ns)*	<τ> (ns)	λ_{em}^{max} (nm)	FWHM (ns)
BC-422Q 1%	0.78 (67) + 3.05 (32)	1.52	360	2.05
BC-422Q 2%	0.81 (73) + 3.08 (27)	1.42	402	1.96
PVT *p*-Q 0.3	1.71 (52) + 11.6 (48)	6.46	370	2.58
PVT *p*-Q 0.6	1.50 (59) + 9.93 (41)	4.69	370	2.52
PVT *p*-Q 1.0	1.52 (66) + 8.41 (34)	3.86	370	2.52
PVT *p*-Q 0.6 B 0.6	1.23 (63) + 8.05 (37)	3.86	370	2.25
PS *p*-T 2 B 2	0.81 (48.5) + 4.09 (51.4)	2.50	410	2.08
PS 4-Br-*p*-T 0.5	0.56 (50) + 2.90 (34.9) + 10.9 (15.1)	2.95	400	1.71

PS 4-Br-*p*-T 1.0	0.99 (49.75) + 5.38 (50.25)	3.19	400	2.14
PS 4-Br-*p*-T 1.5	0.53 (46.5) + 2.80 (36.1) + 11.8 (17.4)	3.31	400	1.71
PS 4-Br-*p*-T 3.5	0.882 (73.9) + 4.00 (26.1)	1.69	400	2.00

* PVT: poly(vinyltoluene), PS: polystyrene, *p*-T: *p*-terphenyl, *p*-Q: *p*-quaterphenyl, 4-Br-*p*-T: 4-bromo-*p*-terphenyl, B: benzophenone. The numeral values of the first row are for the weight concentrations

Among the scintillators listed in Table 4, the fastest formulations were compared in terms of radioluminescence spectra. Thus, each scintillator was exposed to a beta emitting $^{90}Sr/^{90}Y$ radioactive source, and their photoluminescence integral was compared with the same commercial plastics BC-422Q 1% and 2%. Table 5 gives the radioluminescence emission maximum (whose spectra are also given Figure 2), the normalized emission integral against BC-422Q 1% and the corresponding relative light yield, and another parameter we have recently introduced. This is the light intensity given by the combination of the pulse shape with the pulse amplitude, expressed in ph/MeV/ns.[2] The relative light yield was taken by pulse height spectrum using a ^{137}Cs gamma ray source using a standard setup.

Table 5 Radioluminescence performances of selected plastic scintillators. All scintillators are with dimension Φ 49 mm h 10 mm

Composition*	$\lambda_{radiolum.}^{max}$ ± 2 (nm)	Radioluminescence vs. BC-422Q 1% (%)	Light yield ϕ vs. BC-422Q 1% (ph/MeV)	ϕ/<τ> (ph/MeV/ns)
BC-422Q 1%	400	100	1700	1118
BC-422Q 2%	406	56	290	204
PVT *p*-Q 0.3	394	140	1940	300
PVT *p*-Q 0.6	402	118	1310	279
PVT *p*-Q 1.0	398	229	2840	735
PVT *p*-Q 0.6 B 0.6	396	87	610	158
PS 4-Br-*p*-T 1.0	394	52	700	219
PS 4-Br-*p*-T 3.5	396	90	1870	1106

* See Table 4 for abbreviations

For all compounds, a strong dependence of the decay time with the primary fluorophore's concentration is observed. Whereas PPO-based plastics have faster decays for low concentrations,[9] herein *p*-quaterphenyl plastics are accelerated when increasin the concentration. The case of 4-bromo-*p*-terphenyl is more subtle. The decay lies between 2.95 ns and 3.31 ns between 0.5 and 1.5 wt%. At 3.5 wt%, the decay time and the light yield as well show a dramatic improvement, until reaching the performances of BC-422Q 1%, but with no quencher inside. It is noteworthy that at so high concentration 4-Br-*p*-T did not dissolve entirely as small aggregates are still visible. Even if not homogenous, this plastic scintillator could therefore become a suitable alternative to BC-422Q 1% for use with a long-term stability requirement because it does not embed any volatile quencher.

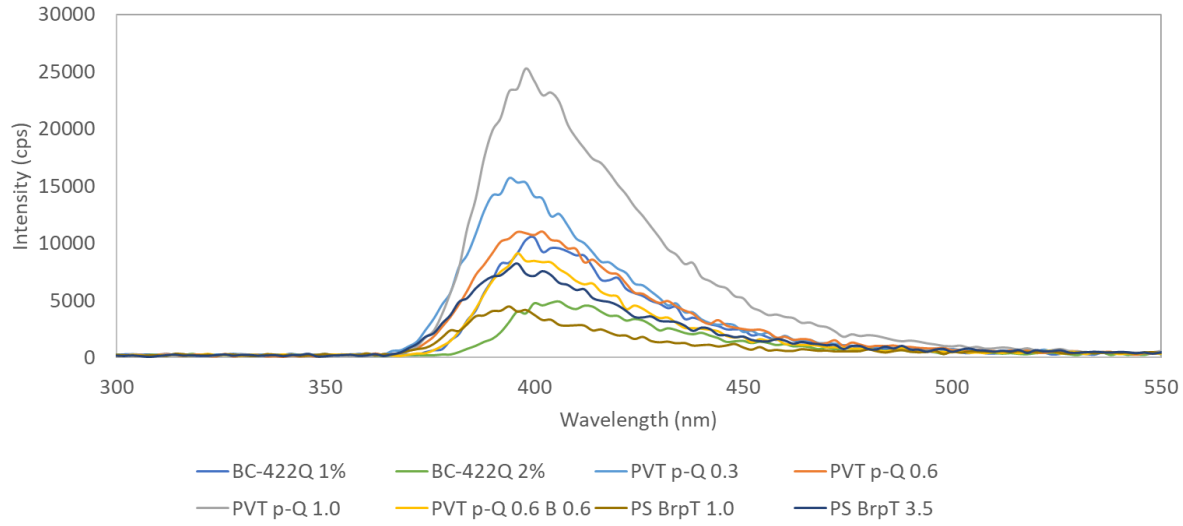
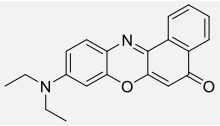


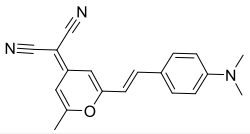
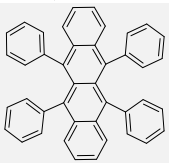
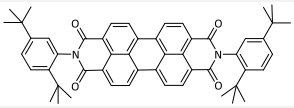
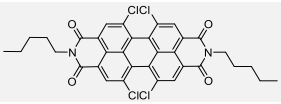
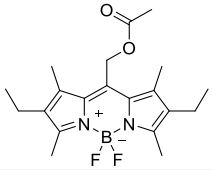
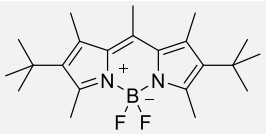
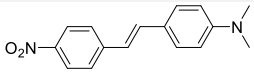
Figure 2 $^{90}Sr/^{90}Y$ radioluminescence of binary mixtures compared with commercial plastics

Matrix + secondary fluorophore mixtures

Intrinsically red-emitting fluorophores present slower decay times than UV-emitting fluorophores as a linear dependence of lifetime with the emission wavelength is predicted.[6] The same procedure as for primary fluorophores has been repeated, that is to say dissolving at low concentrations known red emitting fluorophores that are soluble in toluene, and to check their photoluminescence decay time thanks to TCSPC. The results are given Table 6. Preliminary studies have shown that polar fluorophores could be added at rather high concentration to give fast decaying liquid scintillators.[28] We decided to withdraw this strategy since the as-prepared scintillators with such high concentrations must present very strong self-absorption. Nile red was our primary candidate,[9] despite its long decay time (27.3 ns). Rubrene was first used by Berlman et al.,[7] the two perylenedicarboximide and the two pyrromethene derivatives that have been tested revealed to be too long-decaying, and the best observations were obtained with 4-(dicyanomethylene)-2-methyl-6-(4-dimethylaminostyryl)-4*H*-pyran (DCM) and 4-dimethylamino-4'-nitrostilbene (DANS). On side experiments, xanthene family (Eosin Y, Erythrosin B, Rhodamine derivatives) were tested but displayed poor solubility in polar media such as toluene, polystyrene or poly(vinyltoluene), even at the very low content we are looking at, typically 0.03 wt%. A second strategy was thus developed but not presented herein. Copolymers made from styrene and highly polar monomers were prepared along with the xanthene derivative to be analyzed. However after several week the materials usually degraded, deformed and became cloudiness. This degradation was however not mentioned in literature precedents.[3,12]

Table 6 Main photophysical characteristics of red-emitting molecules dissolved at 0.03 wt% in air-saturated toluene solutions (λ_{ex} = 368 nm; $\lambda_{obs} = \lambda_{em}^{max}$)

Number	Molecule	Structure	λ_{em}^{max} (nm)	τ (ns)
1	Nile red		610	5.18

2	*DCM* 4-(Dicyanomethylene)-2-methyl-6-(4-dimethylaminostyryl)-4*H*-pyran		550	0.95
3	Rubrene		584	27.3
4	*N,N′*-Bis(2,5-di-*tert*-butylphenyl)-3,4,9,10-perylenedicarboximide		580	6.6
5	*N,N′*-Bis-*n*-pentyl-1,6,7,12-tetrachloro-3,4,9,10-perylenedicarboximide		596	11.4
6	*Pyrromethene 605* Difluoro[2-(4-ethyl-3,5-dimethyl-1*H*-pyrrol-2-yl-κ*N*)-2-(4-ethyl-3,5-dimethyl-2*H*-pyrrol-2-ylidene-κ*N*)ethyl acetato])boron		586	12.4
7	*Pyrromethene 597* Difluoro(4-(1,1-dimethylethyl)-2-{1-[4-(1,1-dimethylethyl)-3,5-dimethyl-2*H*-pyrrol-2-ylidene-*N*]ethyl}-3,5-dimethyl-1*H*-pyrrol-2-ylidene-*N*]ethyl}-3,5-dimethyl-1*H*-pyrrolato-*N*)boron		608	13.8
8	*DANS* *Trans*-4-dimethylamino-4'-nitrostilbene		560	3.28

DCM is a molecule that exhibits considerable variability of its photoluminescence response regarding the polarity of the solvent it is dissolved in. DCM was already mentioned as a potential shifter for polystyrene-based scintillators.[29] Photoluminescent literature precedents[30] as well as laboratory measurements are resumed in Table 7. It turns out that in apolar solvent DCM is extremely fast-decaying, with an interesting emission wavelength for our given application ($\lambda_{\mathrm{em}}^{\max} \approx 550\ \mathrm{nm}$), albeit at the expense of the quantum yield, toluene being the best example of such behavior. Accordingly, DCM in styrene was also tested; it turns out that the observed 0.95 ns decay time must be limited by the timing resolution due to the pulse width excitation of our spectrofluorometer, so the decay time of DCM in styrene must be taken with caution. Experimental measurements in PMMA are in well agreement with literature precedents (lines 2 and 1, respectively). Unfortunately, plastic rigidity increases the photoluminescence decay time of DCM – whatever its concentration – towards a 3.8 ns value.

Table 7 Comparison of relevant photophysical data of DCM under various conditions

Matrix		**$\lambda_{\mathrm{em}}^{\max}$ (nm)**	**τ (ns)**	**Quantum yield**
PMMA	*Bibliography*	550	2.0	0.76
PMMA	*Measurement*	550	2.63	n.d.
Toluene	*Bibliography*	567	0.02	0.08
Styrene	*Measurement*	550	0.95	n.d.
Polystyrene	*Measurement*	550	3.80	n.d.

n.d.: not determined

The second molecule that is potentially interesting is 4-dimethylamino-4'-nitrostilbene (usually abbreviated as DANS), known as a push-pull chromophore.[31] To the best of our knowledge DANS has never been used in the scintillation field. The absorption maximum of a 0.002 wt% of DANS in toluene (i.e. 7.45 10^{-5} mol.L^{-1}) is located at 437 nm, with a calculated absorption molar coefficient of 22600 L.mol^{-1}.cm^{-1} (literature 447 nm and 26630 L.mol^{-1}.cm^{-1} in chlorobenzene[32]). This last value is adequate for a secondary fluorophore role and falls between 9,10-diphenylanthracene (ε 14000 L.mol^{-1}.cm^{-1}, cyclohexane[33]) and POPOP (ε 47000 L.mol^{-1}.cm^{-1}, cyclohexane[33]) which are two wavelength shifters particularly used in scintillation. DANS displays a maximum of emission equal to 560 nm and a photoluminescence decay time of 3.28 ns at 0.002 wt% in toluene. This decay time value looks long compared with the 0.94 ns value for its lifetime reported in the literature.[32] This fast decay induces a low photoluminescence quantum yield (0.10 in chlorobenzene[32]), which may be reduced by a twisted intramolecular charge transfer. We also noticed that in toluene, this molecule is also sensitive to traditional quenchers, as can be seen in Table 8. Figure 3 gives the photoluminescence decay profiles of seven liquid scintillators being quenched with either benzophenone, piperidine or the Hünig's base at concentrations of 1.6 wt% or 4.8 wt%. It was unexpected to see appearing an afterglow for "quenched" scintillators with benzophenone. In that case, not only the prompt photoluminescence is affected but a delayed photoluminescence appears. This behavior is still unclear to our eyes. On the other hand, both piperidine and Hünig's base were efficient quenchers, with a quenching efficiency dependent with the quencher concentration, at least for the two studied concentrations. Figure 4 shows a Time-Resoled Emission Spectroscopy spectrum of DANS in toluene and quenched by Hünig's base. As such, the emission characteristics are perfect for our aimed application. Thus, DCM and DANS are selected as potent wavelength-shifters for the design of red and fast plastic scintillators.

Table 8 Quenching of trans*-4-dimethylamino-4'-nitrostilbene with various quenchers. Solvent toluene. λ_{ex} = 368 nm; λ_{obs} = 560 nm*

Quencher	Concentration (wt%)	τ (ns)	<τ> (ns)	FWHM ± 0.05 (ns)
-	0	3.28		5.00
Benzophenone	1.6	3.37		4.78
Benzophenone	4.8	3.44 (89.1) + 61.1 (10.9)	9.72	4.72
Piperidine	1.6	2.02		3.13
Piperidine	4.8	0.91 (72.8) + 2.39 (27.2)	1.31	2.25
Hünig's base	1.6	2.16		3.24
Hünig's base	4.8	1.17 (91.8) + 5.14 (8.2)	1.50	2.41

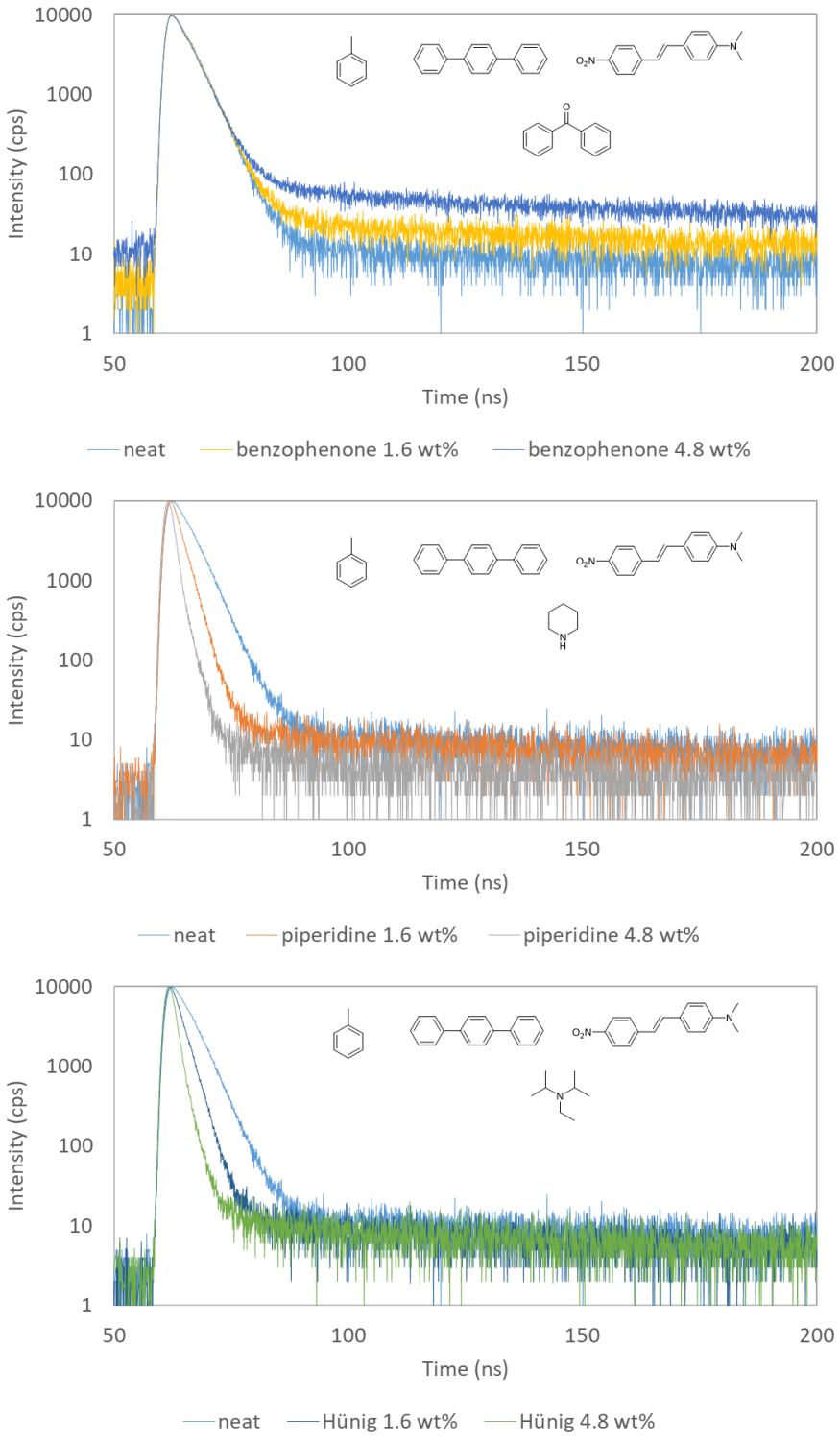


Figure 3 Photoluminescence quenching of a plastic scintillator composed of PS + p-terphenyl 1.5 wt% + DANS 0.01 wt% with different amounts of benzophenone (top), piperidine (middle) or Hünig's base (bottom). The same unquenched, reference material is added on each figure (τ_{ex} = 274 nm; τ_{obs} = 560 nm).

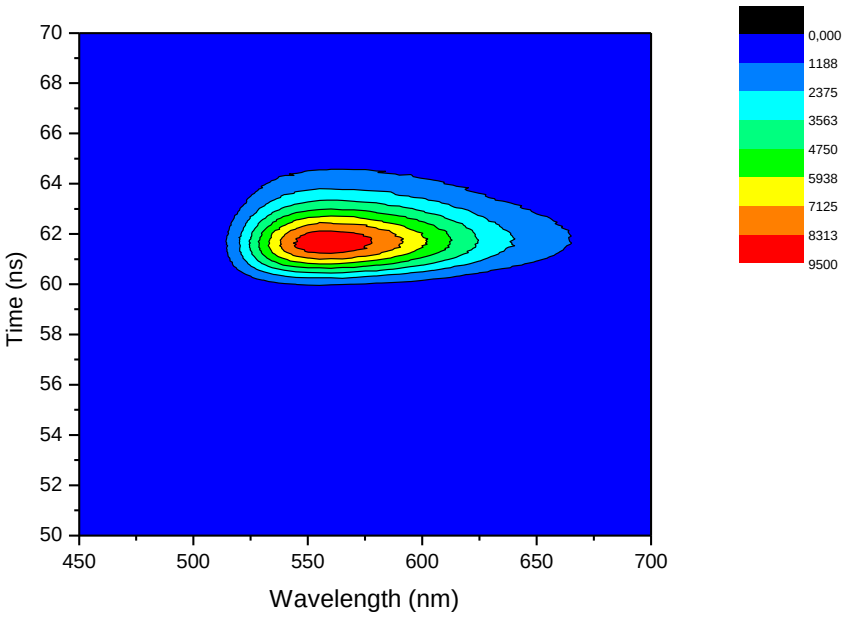


Figure 4 Time-Resolved Emission Spectroscopy of 0.03 wt% 4-dimethylamino-4'-nitrostilbene in toluene, quenched with 5 wt% of Hünig's base. τ_{mean} = 1.50 ns (λ_{ex} = 368 nm)

Full red-and-fast plastic systems

To resume, *p*-terphenyl or its 4-brominated derivative have been chosen as primary fluorophores, when DCM and 4-dimethylamino-4'-nitrostilbene can be useful as secondary fluorophores. Plastic scintillators were thus prepared, starting from polystyrene as the matrix. In addition, several other secondary fluorophores that were presented in Table 6 were also benchmarked. All secondary fluorophores were tested at three different weight concentrations, from 0.01 up to 0.05 wt%. The results are summarized in Table 9.

Table 9 Photoluminescence and scintillation properties of red and fast plastic scintillators compared with BC-430 and BC-422Q 1%. For the TCSPC values: λ_{obs} = 560 nm. All scintillators are with dimension Φ 49 mm h 30 mm, except BC-430 which is Φ 50 mm h 50 mm and BC-422Q 1% which is Φ 50 mm h 15 mm

	Plastic scintillator[a]	λ_{em}^{max} (nm)[b]	τ (ns) λ_{ex} 274 nm	FWHM ± 0.11 (ns)	ϕ (ph/MeV)[c]	ϕ (ph/MeV)[d]	ϕ/<τ> (ph/MeV/ns)[e]
	BC-430	580	12.5	23.00	6900	6900	552
	BC-422Q 1%	380	1.52	2.05	n.d.[f]	1700	1118
G55A	PS + *p*-T 1.5 + DCM (**2**) 0.01	564	3.08 (85.5) + 22.1 (14.5)	5.15	1300	640	208
G55B	PS + *p*-T 1.5 + DCM (**2**) 0.03	574	3.27 (89.7) + 22.4 (10.3)	5.27	1500	740	226
G55C	PS + *p*-T 1.5 + DCM (**2**) 0.05	578	3.42 (92.5) + 23.0 (7.5)	5.27	1300	630	184
F187Q	PS + 4-Br-*p*-T 1.5 + DCM (**2**) 0.03 + B 2	560	3.30	2.08	n.d.	360	109
G53A	PS + *p*-T 1.5 + **3** 0.01	582	23.78	25.35	2330	1700	
G53B	PS + *p*-T 1.5 + **3** 0.03	590	27.35	40.71	2500	2000	
G53C	PS + *p*-T 1.5 + **3** 0.05	590	29.19	37.64	2460	2170	
G52A	PS + *p*-T 1.5 + **4** 0.01	578	7.27 (95.3) + 41.8 (4.7)	8.34	3670	3180	

G52B	PS + *p*-T 1.5 + **4** 0.03	582	9.52 (73.15) + 34.9 (26.85)	11.85	4400	2840	
G52C	PS + *p*-T 1.5 + **4** 0.05	592	9.44 (52.65) + 35.0 (47.35)	12.07	3700	2720	
G54A	PS + *p*-T 1.5 + **5** 0.01	582	10.82	12.94	3210	1600	
G54B	PS + *p*-T 1.5 + **5** 0.03	592	11.44	15.25	3240	1670	
G54C	PS + *p*-T 1.5 + **5** 0.05	596	11.59	13.50	3240	1720	
G57A	PS + *p*-T 1.5 + **7** 0.01	596	12.4	19.20	4250	2360	
G57B	PS + *p*-T 1.5 + **7** 0.03	602	13.8	20.74	4500	2680	
G57C	PS + *p*-T 1.5 + **7** 0.05	604	13.9	22.99	5070	2720	
G59a	PS + *p*-T 1.5 + DANS 0.01	554	4.23	7.13	6280	4020	945
G59b	PS + *p*-T 1.5 + DANS 0.03	570	4.40	7.68	5470	3450	784
G59c	PS + *p*-T 1.5 + DANS 0.05	572	4.68	7.90	5480	3170	677

[a] PS: polystyrene, *p*-T: *p*-terphenyl, 4-Br-*p*-T: 4-bromo-*p*-terphenyl, DCM: 4-(dicyanomethylene)-2-methyl-6-(4-dimethylaminostyryl)-4*H*-pyran, DANS: *trans*-4-dimethylamino-4'-nitrostilbene, B: benzophenone, P: piperidine, H: Hünig's base. The values of the first row are for the weight concentrations. The numbers in bold font refer to the red-emitting fluorophores described in Table 6.

[b] values in radioluminescence.

[c] estimated by beta-induced pulse height spectroscopy. The relative is calculated by a rule of thumb between BC-430 light yield reference.[34]

[d] estimated by radioluminescence. The relative light yield is calculated by a rule of thumb between BC-430 light yield reference, its radioluminescence integral and the other samples integral.

[e] the light yield recorded from beta-induced pulse spectroscopy was used in this calculation.

[f] n.d.: not determined.

The first observation is the fact the DANS-based scintillators are not as fast as their liquid equivalents, with TCSPC values giving around 4 ns. This was already observed for Nile Red-based scintillators.[9] The radioluminescence spectra show emission wavelengths that are in agreement with the photoluminescence spectra.

The determination of the light output of the scintillators was performed either with a radioluminescence setup (^{90}Sr/^{90}Y excitation) or with a more traditional pulse-height spectrum methodology (^{36}Cl excitation). In both cases, beta emitters were used, and the plastic scintillators were benchmarked against BC-430 commercial plastic. This light output is then divided by the mean decay value, which gives the number of photons per deposited energy per time. This parameter is thus the most important parameter for most applications, and it favors very fast materials. Here, BC-430 and BC-422Q 1% afford 552 and 1118 ph/MeV/ns, respectively. The best results for our prepared scintillators were obtained with the DANS-based scintillators, with a value of the same order of magnitude as for BC-422Q 1%. The weakest materials were the DCM-based, since the quantum yield of DCM in polystyrene is too low.

Having in hand promising materials with the use of DANS, it is noteworthy that this molecule can be quenched by amines or benzophenone as shown before. Thus, the same PS + *p*-terphenyl + DANS (0.01 wt%) were prepared with three different amounts of benzophenone, piperidine or Hünig's base. Unfortunately, the time stability was not in favor to the scintillators loaded with the two amines. After almost 18 months of preparation, the materials suffered from intense visual degradation (Figure 5). The DANS molecule probably reacted with the amines since the emission spectra are totally different from the pristine materials. This visual information was confirmed by fluorescence spectroscopy, where all scintillators had almost the same fluorescence spectrum immediately after production, and Figure 6 shows their chemical degradation. The blue shift of the emission spectrum is confirmed for

the scintillators containing the amines only, with emission maxima located close to 470 nm for the two highest quenched scintillators (P4.8 and H4.8), when the neat or even the benzophenone-quenched scintillators keep their emission maxima close to 560 nm.

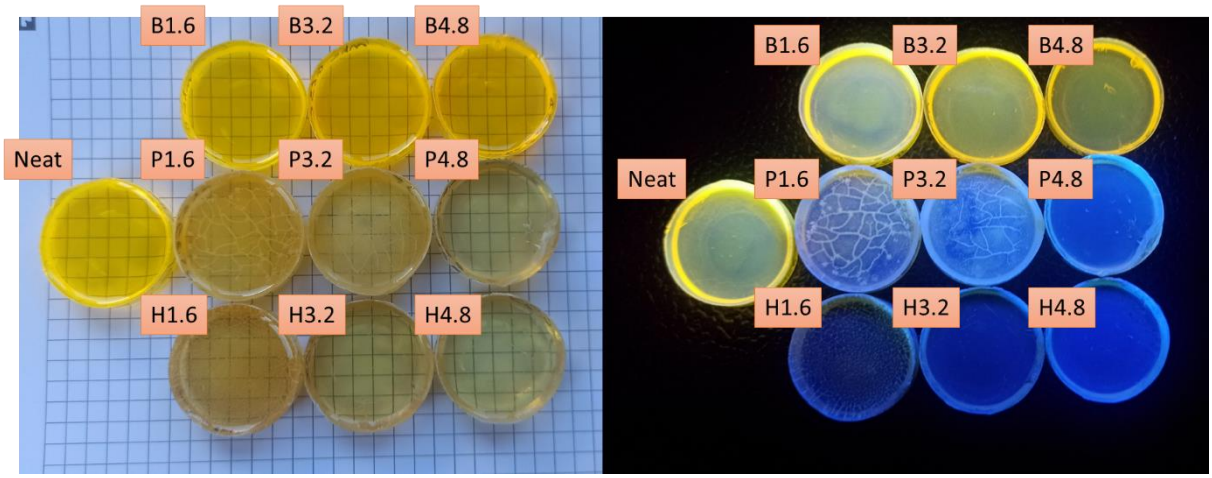


Figure 5 Scintillators composed of polystyrene containing p-terphenyl, DANS and quenchers, under visible light (left) and 368 nm UV (right), pictured 18 months after preparation. B, P and H stand for Benzophenone, Piperidine and Hünig's base, respectively with their added concentration.

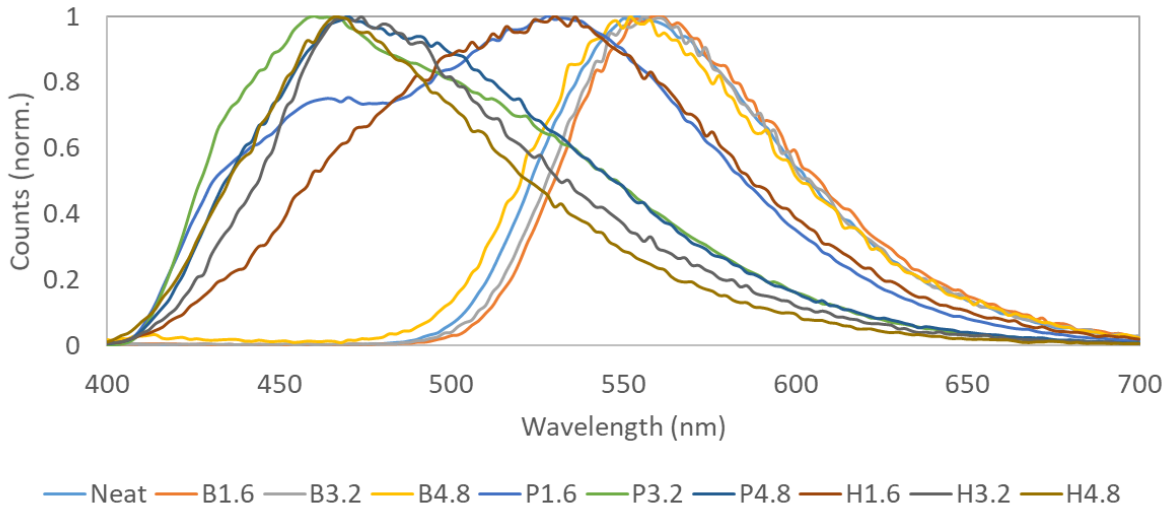


Figure 6 Fluorescence spectroscopy of p-terphenyl + DANS scintillators quenched with various amounts of quenchers: benzophenone (B series), piperidine (P series) or Hünig's base (H series). λ_{ex} = 370 nm.

4. Conclusions

Red and fast plastic scintillators have been decomposed into individual elements to better optimize their formulation. As a violet-emitting plastic scintillator, highly concentrated 4-bromo-*p*-terphenyl in polystyrene displays equal performances to BC-422Q 1%, but without the use of any quencher. This would allow a more stable material compared to previous studies about the time stability of quenched scintillators.[22] More than 4-bromo-*p*-terphenyl, several other molecules may act as nanosecond-range, UV-emitting fluorophore in a polymer matrix: oligophenylene family and several oxadiazoles among other.

It was awaited that adding a wavelength-shifter increases the decay time. However, two different orange-emitting molecules could fit our purpose: DCM and *trans*-4-dimethylamino-4'-nitrostilbene. DCM leads to very fast scintillators but with poor scintillating properties. *Trans*-4-dimethylamino-4'-nitrostilbene whose first use in the scintillation field (at least to the best of our knowledge) is described herein allocates both fastness and high light yield. For both fluorophores, mean decay time and FWHM in the range of 4 ns are obtained, which grant them the fastest scintillators with emission wavelength more than 550 nm ever described. Interestingly, *p*-terphenyl and DANS that are our final choice are both sensitive to quenching with amines. Unfortunately, these scintillators were not stable with time when being quenched with piperidine or *N,N*-diisopropylethylamine. This work falls within recent efforts to find fast and red scintillators, whether organics or inorganics.[35]

Conflict of interest

The author declares that he has no known competing financial interests or personal relationships that could have appeared to influence the work reported in this paper.

Acknowledgements

The author acknowledges the financial support of the Cross-Disciplinary Program on Instrumentation and Detection of CEA, the French Alternative Energies and Atomic Energy Commission.

References

[1] Dujardin, C.; Hamel, M. In *Plastic Scintillators: chemistry and applications*; Hamel, M., Ed.; Springer Nature: Cham, 2021, pp. 3-33. https://doi.org/10.1007/978-3-030-73488-6_1

[2] Hamel, M.; Pjatkan, R.; Burešová, H. *Nucl. Instr. Methods A* **2020**, *955*, 163294. https://doi.org/10.1016/j.nima.2019.163294

[3] Franks, L. A.; Lutz, S.; Lyons, P. B. *IEEE Trans. Nucl. Sci.* **1978**, *NS-25*, 1024-1026. https://doi.org/10.1109/TNS.1978.4329455

[4] Beddar, S.; Tendler, I.; Therriault-Proulx, F.; Archambault, L.; Beaulieu, L. In *Plastic Scintillators: chemistry and applications*; Hamel, M., Ed.; Springer Nature: Cham, 2021, p 425-460. https://doi.org/10.1007/978-3-030-73488-6_12

[5] Hamel, M.; Turk, G.; Rousseau, A.; Darbon, S.; Reverdin, C.; Normand, S. *Nucl. Instr. Methods A* **2011**, *660*, 57-63. https://doi.org/10.1016/j.nima.2011.08.062

[6] Cahill, P. A. *Radiat. Phys. Chem.* **1993**, *41*, 351-363. https://doi.org/10.1016/0969-806X(93)90072-3

[7] Berlman, I. B.; Ogdan, Y. *Nucl. Instr. Methods* **1980**, *178*, 411-413. https://doi.org/10.1016/0029-554X(80)90819-8

[8] Montbarbon, E.; Amiot, M.-N.; Tromson, D.; Gaillard, S.; Frangville, C.; Woo, R.; Bertrand, G. H. V.; Pansu, R. B.; Renaud, J.-L.; Hamel, M. *Phys. Chem. Chem. Phys.* **2017**, *19*, 28105-28115. https://doi.org/10.1039/C7CP04034B

[9] Hamel, M. ; Trocmé, M. ; Rousseau, A. ; Darbon, S. *J. Lumin.* **2017**, *190*, 511-517. https://doi.org/10.1016/j.jlumin.2017.06.012

[10] Tanaka, K.; Yanagida, T.; Hirose, A.; Yamane, H.; Yoshii, R.; Chujo, Y. *RSC Adv.* **2015**, *5*, 966563. https://doi.org/10.1039/C5RA20459C

[11] Ponomarenko, S. A.; Surin, N. M.; Borshchev, O. V.; Luponosov, Y. N.; Akimov, D. Y.; Alexandrov, I. S.; Burenkov, A. A.; Kovalenko, A. G.; Stekhanov, V. N.; Kleymyuk, E. A.; Gritsenko, O. T.; Cherkaev, G. V.; Kechek'yan, A. S.; Serenko, O. A.; Muzafarov, A. M. *Sci. Rep.* **2014**, *4*, 6549. https://doi.org/10.1038/srep06549

[12] Huijun, Y.; Xiangtuo, W.; Yuying, J.; Yuanli, Z. *J. Lumin.* **1984**, *31-32*, 833-835. https://doi.org/10.1016/0022-2313(84)90140-6

[13] Dalla Palma, M.; Quaranta, A.; Marchi, T.; Collazuol, G.; Carturan, S.; Cinausero, M.; Degerlier, M.; Gramegna, F. *IEEE Trans. Nucl. Sci.* **2014**, *61*, 2052-2058. https://doi.org/10.1109/TNS.2014.2302036

[14] Gandini, M.; Villa, I.; Beretta, M.; Gotti, C.; Imran, M.; Carulli, F.; Fantuzzi, E.; Sassi, M.; Zaffalon, M.; Brofferio, C.; Manna, L.; Beverina, L.; Vedda, A.; Fasoli, M.; Gironi, L.; Brovelli, S. *Nat. Nanotechnol.* **2020**, *15*, 462-468. https://doi.org/10.1038/s41565-020-0683-8

[15] Huijun, Y. *He Dianzixue Yu Tance Jishu* **1990**, *10*, 353-355.

[16] Adadurov, A. F.; Zhmurin, P. N.; Lebedev, V. N.; Kovalenko, V. V. *Nucl. Instr. Methods A* **2010**, *621*, 354-357. https://doi.org/10.1016/j.nima.2010.04.055

[17] Ma, W.; Su, Y.; Zhang, Q.; Deng, C.; Pasquali, L.; Zhu, W.; Tian, Y.; Ran, P.; Chen, Z.; Yang, G.; Liang, G.; Liu, T.; Zhu, H.; Huang, P.; Zhong, H.; Wang, K.; Peng, S.; Xia, J.; Liu, H.; Liu, X.; Yang, Y. (M.) *Nat. Mater.* **2021**. https://doi.org/10.1038/s41563-021-01132-x

[18] Sytnik, A.; Kasha, M. *Radiat. Phys. Chem.* **1993**, *41*, 331-349. https://doi.org/10.1016/0969-806X(93)90071-2

[19] Tanaka, K.; Yanagida, T.; Yamane, H.; Hirose, A.; Yoshii, R.; Chujo, Y. *Bioorg. Med. Chem. Lett.* **2015**, *25*, 5331-5334. https://doi.org/10.1016/j.bmcl.2015.09.037

[20] Shakirova, J. R.; Grachova, E. V.; Melekhova, A. A.; Krupenya, D. V.; Gurzhiy, V. V.; Karttunen, A. J.; Koshevoy, I. O.; Melnikov, A. S.; Tunik, S. P. *Eur. J. Inorg. Chem.* **2012**, 4048-4056. https://doi.org/10.1002/ejic.201200362

[21] Montbarbon, E.; Sguerra, F.; Bertrand, G.H.V.; Magnier, É.; Coulon, R.; Pansu, R. B.; Hamel, M. *Chem. – Eur. J.* **2016**, *22*, 12074-12080. http://dx.doi.org/10.1002/chem.201601749

[22] Ebran, A.; Taieb, J.; Belier, G.; Chatillon, A.; Laurent, B.; Martin, J.-F.; Pellereau, E. *Nucl. Instr. Methods A* **2013**, *728*, 40-46. http://dx.doi.org/10.1016/j.nima.2013.06.021

[23] Moszyński, M. *Nucl. Instr. Methods* **1976**, *134*, 77-85. https://doi.org/10.1016/0029-554X(76)90126-9

[24] Moszyński M.; Bengtson, B. *Nucl. Instr. Methods* **1979**, *158*, 1-31. https://doi.org/10.1016/S0029-554X(79)90170-8

[25] https://www.horiba.com/us/en/scientific/products/fluorescence-spectroscopy/lifetime/tcspc-components/nanoled/nanoled-618/

[26] Berlman, I. B.; Lutz, S. S.; Flournoy, J. M.; Ashford, C. B.; Franks, L.A.; Lyons, P. B. *Nucl. Instr. Methods* **1984**, *225*, 78-84. https://doi.org/10.1016/0167-5087(84)91340-1

[27] Andreeshchev, E. A.; Avedisyan, V. S.; Veronyan, S. M.; Zyablin, V. L.; Kovyrzina, K. A.; Kushakevich, Y. P.; Rozman, I. M.; Shoniya, V. M. *Instr. Exp. Techn.* **1988**, *31*, 593-595. Translated from *Prib. Tekh. Eksp.* **1988**, 67-68.

[28] Lutz, S. S.; Franks, L. A.; Flournoy, J. M. *Nucl. Instr. Methods* **1982**, *193*, 623-629. https://doi.org/10.1016/0029-554X(82)90260-9

[29] Zheng, H.; Baumbaugh, B.; Gerig, A.; Hurlbut, C;. Kauffman, J.; Marchant, J.; Pla-Dalmau, A.; Reynolds, K.; Ruchti, R.; Warchol, J.; Wayne, M. *AIP Conf. Proc.* **1998**, *450*, 371-380. https://doi.org/10.1063/1.56945

[30] Bondarev, S. L.; Knyukshto, V. N.; Stepuro, V. I.; Stupak, A. P.; Turban, A. A. *J. Appl. Spectrosc.* **2004**, *71*, 194-201. Translated from *Zh. Prikl. Spektrosk.* **2004**, *71*, 179-186. https://doi.org/10.1023/B:JAPS.0000032874.60100.a0

[31] Muniz-Miranda, F.; Pedone, A.; Muniz-Miranda, M. *Spectrochim. Acta, Part A* **2018**, *190*, 33-39. https://doi.org/10.1016/j.saa.2017.08.072

[32] Papper, V.; Pines, D.; Likhtenshtein, G.; Pines, E. *J. Photochem. Photobiol. A* **1997**, *111*, 87-96. https://doi.org/10.1016/S1010-6030(97)00234-7

[33] Taniguchi, M.; Lindsey, J. S. *Photochem. Photobiol.* **2018**, *94*, 290-327. https://doi.org/10.1111/php.12860

[34] https://www.crystals.saint-gobain.com/sites/imdf.crystals.com/files/documents/bc430-data-sheet.pdf

[35] Li, Y.; Chen, L.; Gao, R.; Liu, B.; Zheng, W.; Zhu, Y.; Ruan, J.; Ouyang, X.; Xu, Q. *ACS Appl. Mater. Interfaces* **2021**, *14*, 1489-1495. https://doi.org/10.1021/acsami.1c21055